Author Manuscript

Author Manuscript

Author Manuscript

Author Manuscript

HHS Public Access

Author manuscript

Brain Behav Immun. Author manuscript; available in PMC 2021 July 01.

Published in final edited form as:

Brain Behav Immun. 2020 July ; 87: 543–555. doi:10.1016/j.bbi.2020.01.026.

let-7g counteracts endothelial dysfunction and ameliorating neurological functions in mouse ischemia/reperfusion stroke model

David L. Bernstein[1], **Sachin Gajghate**[1], **Nancy L. Reichenbach**[1], **Malika Winfield**[1], **Yuri Persidsky**[1,2], **Nathan A. Heldt**[1], **Slava Rom**[1,2]

[1]Department of Pathology and Laboratory Medicine, Temple University, Philadelphia, PA 19140, USA

[2]Center for Substance Abuse Research, Lewis Katz School of Medicine, Temple University, Philadelphia, PA 19140, USA

Abstract

Stroke is a debilitating disease, accounting for almost 20% of all hospital visits, and 8% of all fatalities in the United States in 2017. Following an ischemic attack, inflammatory processes originating from endothelial cells within the brain microvasculature can induce many toxic effects into the impacted area, from both sides of the blood brain barrier (BBB). In addition to increased BBB permeability, impacted brain microvascular endothelial cells can recruit macrophages and other immune cells from the periphery and can also trigger the activation of microglia and astrocytes within the brain. We have identified a key microRNA, let-7g, which levels were drastically diminished as consequence of transient middle cerebral artery occlusion (tMCAO) *in vivo* and oxygen-glucose deprivation (OGD) *in vitro* ischemia/reperfusion conditions, respectively. We have observed that let-7g* liposome-based delivery is capable of attenuating inflammation after stroke, reducing BBB permeability, limiting brain infiltration by $CD3^+CD4^+$ T-cells and $Ly6G^+$ neutrophils, lessening microglia activation and neuronal death. These effects consequently improved clinical outcomes, shown by mitigating post-stroke gait asymmetry and extremity motor function. Due to the role of the endothelium in propagating the effects of stroke and other inflammation, treatments which can reduce endothelial inflammation and limit ischemic damage and improving recovery after a stroke are required. Our findings demonstrate a critical link

Corresponding author: Slava Rom, PhD, Temple University School of Medicine, Department of Pathology and Laboratory Medicine, 3500 N. Broad Street, Medical Education and Research Building, room 842, Philadelphia, PA 19140. Phone: (215) 707-9412; Fax: (215) 707-5255, srom@temple.edu.

Author contributions

David L. Bernstein - data acquisition and analysis, drafting, revising and final approval article, Sachin Gajghate - data acquisition and analysis, revising and final approval article, Nancy L. Reichenbach - data acquisition and analysis, revising and final approval article, Malika Winfield - data acquisition and analysis, revising and final approval article, Nathan A. Heldt- data acquisition and analysis, revising and final approval article, Yuri Persidsky - data interpretation, revising article, and final approval, Slava Rom - conception and design, data acquisition, analysis and interpretation, drafting and revising article, and final approval.

Publisher's Disclaimer: This is a PDF file of an unedited manuscript that has been accepted for publication. As a service to our customers we are providing this early version of the manuscript. The manuscript will undergo copyediting, typesetting, and review of the resulting proof before it is published in its final form. Please note that during the production process errors may be discovered which could affect the content, and all legal disclaimers that apply to the journal pertain.

Disclosure/Conflict of Interest

None

Author Manuscript Author Manuscript Author Manuscript Author Manuscript

between the CNS inflammation and the immune system reaction and lay important groundwork for future stroke pharmacotherapies.

Keywords

stroke; blood brain barrier; ischemia/reperfusion; leukocyte infiltration; microRNA

Introduction

Stroke is a debilitating disease in the developed and developing world. In the United States in 2017, stroke was the #3 cause of death, leading to almost 150,000 deaths, over 10 million hospital visits, and costing an estimated 219 billion dollars (Yang et al., 2017a). Stroke is a prominent cause of long-term disability in humans. Four out of five stroke survivors have walking impairments and, despite rehabilitation efforts, 25% of survivors have residual gait deficiencies which disturb their daily activities and mobility (Li et al., 2018a; Parkkinen et al., 2013; Wang et al., 2008).

In spite of the prominence as a leading cause of death and disability, few treatments currently exist for the treatment of stroke. Tissue plasminogen activator (tPA) and mechanical thrombectomy remain the only clinical approaches. While both are effective at removing the clot and restoring perfusion (Nour et al., 2013), they offer little to no protection of the brain from ischemic and reperfusion injury arising from inflammation (Ahnstedt et al., 2016; Chen et al., 2018; Nour et al., 2013). Further, both treatments have limited “clinical windows” in which they will be effective at preserving brain tissue (Chen et al., 2018; Kepplinger et al., 2016; Knecht et al., 2018), and there remains some debate surrounding the optimal timepoint for tPA treatment.

Brain microvascular endothelial cells (BMVECs) assure the tightness of blood brain barrier (BBB) and possess many unique elements which distinguish them from other vascular endothelial cells, such as specialized tight junction proteins, and a significantly higher expression of monoamine oxidase A (Meresse et al., 1989; Uwamori et al., 2019). During the development of stroke, inflammatory cytokines, such as CCL5 and MCP-1 are released from the brain microvasculature (Conductier et al., 2010; Zhang et al., 2007). These cytokines travel through the bloodstream to the organs of the immune system, where they begin to activate immune cells, and trigger neutrophil release (von Vietinghoff and Ley, 2009). Activated neutrophils migrate to the site of injury, reaching a peak within 24 hours (de Oliveira et al., 2016). Their accumulation worsens the local microvascular environment (del Zoppo, 2009; del Zoppo et al., 1998) and leads to the production of other cytokines, which ultimately recruit monocytes, macrophages and cytotoxic T cells from the periphery (Beurel, 2011). In addition, the changes to the endothelial cells result in activation of microglia in the CNS (Ju et al., 2018) and induce pericyte detachment (Yang et al., 2017b), further damaging the BBB. In the initial hours and days following stroke, all these inflammatory processes converge on the brain endothelial cells, which, having already been damaged by hypoxia and reperfusion cascade events, begin to weaken and die, promoting immune cell infiltration and glial activation in the CNS, and further worsening the damage

Author Manuscript Author Manuscript Author Manuscript Author Manuscript

from the ischemic attack. BMVECs have become the target of many proposed stroke pharmacotherapies, as they represent a major interface between the CNS and peripheral immune/inflammatory responses (del Zoppo, 2009; Faraco et al., 2017; Minami, 2011; Posada-Duque et al., 2014). Furthermore, these cells lay at the luminal side of the BBB, making them more readily accessible to treatments, compared with targets within the CNS. Combined difficulty and considerable risks associated with use of compounds which cross the BBB, treatment of neuroinflammation with molecules improving BMVEC functions remains a highly plausible therapeutic strategy for stroke.

Recently, we have identified a number of microRNAs (miRs), miR-98 and let-7g*, belonging to the let-7 family, which are significantly downregulated in endothelium following inflammatory insult. The let-7 gene was originally discovered in the early 2000's in *C. elegance* as lethal-7 (for being crucial during development), hence the name, let-7; soon after let-7 was found in many other species (Roush and Slack, 2008). The let-7 family of miRs are present in multiple isoforms and copies across the genome. In mice and humans, 10 of the let-7 miRs (let-7a, b, c, d, e, f, g, i, miR-98 and miR-202) are present in the genome (Roush and Slack, 2008). During miRNA biogenesis, one of the strands of the Dicer reaction's product is loaded into RISC, as mature miR. The other strand which is named the "star strand" is usually degraded (Bartel, 2004; Eder et al., 1991). However, for some miRs, both strands are kept and are loaded into RISC as mature forms. In such a case the mature miR is called for example with let-7g miR, as let-7g-5p and let-7g-3p, or let-7g and let-7g*, respectively. Several of the let-7' miRs in particular (let-7b, let-7g, let-7g*) and miR-98 when *under* expressed, appear to be involved in several inflammation processes, including cardiovascular and endothelial (Bernstein et al., 2019; Liao et al., 2014; Liu et al., 2017; Rom et al., 2015). let-7g has been showed to contribute to maintaining endothelial and vascular function in experimental atherosclerosis, one of the stroke-contributing factors (Liao et al., 2014; Liu et al., 2017). Despite such findings, the role of let-7g in modulating the vascular response to ischemia remains poorly understood. Currently, emerging evidence points to a reduction of let-7g miRNA expression following hypoxic conditions (Li et al., 2019; Zhang et al., 2016). Because let-7g's expression is regulated by a number of cellular elements which are associated with inflammatory states (Brennan et al., 2017) and chemokine release (Quinn and O'Neill, 2014), it is possible that the relative paucity of let-7g during inflammatory conditions, such as stroke, may represent an area in which prompt pharmacological intervention could ameliorate the effects of stroke. Both miRNAs, let-7g and its complimentary sequence let-7g* are originated from the same gene, and potentially both might have a role in stroke or inflammatory processes. Recently our group has demonstrated that overexpression of let-7g* has been shown to be highly neuroprotective and have beneficial effects on vascular tissue, improved endothelial tightness and decreased leukocyte adhesion to and migration across endothelium (Rom et al., 2015). The anti-inflammatory and neuroprotective characteristics of let-7g* (Rom et al., 2015) prompted us to investigate its role in the setting of stroke, since knowledge of the function of let-7g* in ischemia/reperfusion is very limited.

In the current study, we devised a model utilizing liposome-based delivery for increasing let-7g* expression, following ischemic events, both *in vitro* and *in vivo*, utilizing transient middle cerebral artery occlusion (tMCAO) and oxygen-glucose deprivation followed by

Author Manuscript Author Manuscript Author Manuscript Author Manuscript

reperfusion (OGD/R), respectively. We assessed the impacts on cellular function, BBB integrity and permeability, immune cell recruitment, microglial activation, and ultimately on measures of behavior, including improvement in gait after stroke. Taken together, our study is the first to focus on the impact of let-7g* on the propagation of ischemic damage, and introduces a novel mechanism for endothelial-immunological interactions through changes in miRNA expression with a potential development of therapeutic approaches to mitigate post-stroke neurological deficits.

Materials and Methods

Oxygen-Glucose Deprivation (OGD) followed by Re-oxygenation (OGD/R)

Primary BMVECs, isolated from vessels obtained from brain resection tissue (showing no abnormalities) of patients undergoing surgery for treatment of intractable epilepsy, were supplied by Michael Bernas and Dr. Marlys Witte (University of Arizona, Tucson, AZ, USA) and were maintained as described (Rom et al., 2015; Rom et al., 2012; Rom et al., 2013). Ischemia-reperfusion conditions were simulated using an OGD/R protocol (Bernstein et al., 2019; Ku et al., 2016). Cell culture media was replaced with no glucose-containing DMEM (Invitrogen, Life Technologies, Carlsbad, CA, USA) and the plates were positioned in a gas exchange chamber (MIC-101, Billups-Rothenberg, Inc., Del Mar, CA, USA). Anaerobic conditions were accomplished with gas (1% O_2, 5% CO_2, balance N_2) and the plates were left in OGD conditions for a further 2–4 h in the incubator (Bernstein et al., 2019; Ku et al., 2016); medium was then exchanged for re-oxygenation with glucose-containing DMEM and left for 24–76 hr in the incubator.

Animals

All animal experiments were approved by the Temple University Institutional Animal Care and Use Committee and were conducted in accordance with Temple University guidelines, which are based on the National Institutes of Health (NIH) guide for care and use of laboratory animals and with the ARRIVE (Animal Research: Reporting *In Vivo* Experiments) guidelines (study design, experimental procedures, housing and husbandry, statistical methods) (www.nc3rs.org.uk/arrive-guidelines). Eight-week old male C57BL/6 mice were purchased from the Jackson Laboratory (Bar Harbor, ME, USA).

Transient Middle Cerebral Artery Occlusion (tMCAO)

Mice were subjected to 60 min focal cerebral ischemia produced by transient intraluminal occlusion with a monofilament made of 6–0 nylon with a rounded tip (Doccol Corp., Sharon, MA, USA, cat# 602312PK10) into the middle cerebral artery (MCAO) as described previously (Bernstein et al., 2019; Engel et al., 2011; Jin et al., 2010). To achieve transient MCAO, the mice were re-anesthetized and the suture was extracted. Body temperature was monitored throughout surgery with a rectal probe and maintained at 37.0 ± 0.5 °C using a heating pad (Gaymar Industries Inc., Orchard Park, NY, USA). Sham-operated mice were subjected to the same surgical procedure, but the filament was not advanced far enough to occlude the middle cerebral artery. At 96 h after the induction of MCAO, mice were anesthetized with 5% isoflurane and euthanized by cervical dislocation, decapitated, and the brain was collected. To ensure rigor in tMCAO experiments, each mouse was monitored for

Author Manuscript Author Manuscript Author Manuscript Author Manuscript

regional cerebral blood flow (rCBF) before ischemia, during MCAO, and after reperfusion using a Laser Speckle PeriCam PSI System (Perimed AB, Järfälla, Sweden). If rCBF was not reduced to at least 25% of initial level, the animal was excluded from the study and euthanized (Bernstein et al., 2019; Zhang et al., 2007).

Neurological assessment

Neurological score assessment was performed 72 h and 168 h (3 and 7 days, respectively) after the onset of ischemia. Overall neurological improvement was observed in enhanced locomotor activity (measured by total ambulation counts, utilizing "Photobeam Activity System: Home Cage" (San Diego Instruments, San Diego, CA, USA) (Bernstein et al., 2019; Chen et al., 2015; DeVries et al., 2001; Ronca et al., 2015; Winter et al., 2005). The corner test, which is perceptive to sensorimotor and postural symmetries, was used. Mice suffering stroke typically turn toward the affected side (right), while non-affected mice have almost 50–50% left to right turn distribution. All mice tested were allowed to enter a corner with an angle of 30° which required them to turn either to the right or the left to exit the corner. This test was repeated and documented ten times, with a minimum of 30 seconds between trials, and the percentage of right turns out of total turns was calculated (Chen et al., 2015; DeVries et al., 2001; Feng et al., 2017; Ronca et al., 2015; Winter et al., 2005; Zhang et al., 2002). Finally, the paws of the mice were painted with nontoxic paint, and the mice were allowed to walk across a sheet of paper to allow for the analysis of gait to be performed. The resulting footprints allow the determination of static gait parameters (e.g., stride length and toe spread) (Balkaya et al., 2013; Chen et al., 2019; Hetze et al., 2012; Inserra et al., 1998).

Mouse brain microvessel (MV) isolation

Mouse brain MVs were isolated using a protocol based on previously published studies (Bernstein et al., 2019; Chun et al., 2011; Rom et al., 2015). For each preparation, mice (n is described in figure legends) were overdosed with 5% isoflurane and their brains were harvested and placed in 4°C HBSS. The cerebellum, meninges, choroid plexus, brain stem, and large superficial blood vessels were removed. The residual tissue was diced in HBSS (4 ml/gram) and then homogenized using a Potter-Thomas homogenizer (0.25 mm clearance) (Thomas Scientific, Swedesboro, NJ, USA). The homogenate was centrifuged (1000xg for 10 min at 4°C) to remove HBSS, resuspended in 17.5% dextran (Sigma/Aldrich, St. Louis, MO, USA) and centrifuged again to separate the MVs. The MV pellet was resuspended in 1% BSA in HBSS and the supernatant was centrifuged (4000xg for 10 min at 4°C). The MVs from each centrifugation were combined. The MV suspension was passed through a 100-μm nylon mesh filter and then through a 40-μm nylon mesh filter (Corning Life Sciences, Tewksbury, MA, USA). The material retained on the 40-μm nylon mesh filter contained the MVs.

In vitro and *in vivo* miRNA transfection, and Quantitative RT-PCR

Recently, in our laboratory, we have developed a successful BMVEC transfection protocol (Rom et al., 2015). In short, BMVECs were transfected at 2×10^6 cells/ml with miRNA oligos at 50 nM with the Neon™ Transfection System (Invitrogen) according to the manufacturer's instructions. Cells were collected 24, 48, 72 and 96 h after transfection and levels of transfected miRNAs were estimated by qPCR as described below.

Author Manuscript Author Manuscript Author Manuscript Author Manuscript

Short oligonucleotide sequences, such as miRNA or siRNA, can permeate cell membranes. Since miRNA can be degraded if injected in a non-encapsulated form, we used a protocol recently developed in our laboratory (Bernstein et al., 2019; Rom et al., 2015) using a liposome-based miRNA transport system. To generate miRNA-containing liposomes, 5 nmol synthetic miRNA (GE Healthcare Dharmacon, Inc., Lafayette, CO, USA) were mixed with Lipofectamine 2000 (Life Technologies) in RNase and DNase-free water (Life Technologies) per the manufacturer's directions. Lipid-oligo complexes were incubated at room temperature for at least 1 hr and, if required, stored at 4°C overnight. The miRNA-liposome complex was diluted in PBS and 100 μl was injected per mouse. Mice were injected (i.v.) with miRNA-liposomes (Jiang et al., 2012; Larson et al., 2007) 2 hr after tMCAO followed by a second injection 24 h later as described (Bernstein et al., 2019; Rom et al., 2015). To verify efficiency of miRNA delivery into MVs, mouse brains were harvested at different time points (48, 72 and 96 h) following miRNA administration. MVs were isolated and the amount of transfected miRNA was estimated by qPCR as described below. While injection of liposome-miRNA complex resulted in a 3.28-fold increase at 72 hr in MVs and 2.2-fold increase in the brain inlet-7g* miRNA expression was found even 5 days after injection.

Real-time RT-PCR was used to detect the differential expression of target genes. RNA was isolated utilizing the mirVana miRNA extraction kit (Life Technologies). Real-time RT-PCR was performed using the mirVana qRT-PCR miRNA detection kit (Life Technologies) per the manufacturer's protocol as described previously (Rom et al., 2015). PCR primer pairs for reverse transcription and detection of mature miRs were purchased from Life Technologies (hsa-let-7g (hsa-let-7g-3p) and control U6). In general, quantitative real-time RT-PCR (qRT-PCR) on primary BMVEC or isolated MVs was performed on 3 independent experiments using 25 ng of template using the Quantstudio S3 real-time PCR system (Life Technologies). For each sample, qRT-PCR was performed in triplicate. Amplification was analyzed using the ΔΔCt method, using a web-based data analysis tool (SABiosciences, Qiagen Inc., Valencia, CA, USA) by normalization to the corresponding values of housekeeping gene (U6) and fold-change was calculated from the difference between experimental condition and untreated control.

Flow cytometry (FACS) for brain infiltrating leukocytes

Brain infiltrating leukocytes (BIL) and microglia were isolated from infarcted and non-infarcted hemispheres by Percoll/Ficoll centrifugation (Bernstein et al., 2019; Jin and Kim, 2015; Ryg-Cornejo et al., 2013) followed by surface staining with antibodies against mouse CD45 (clone 30-F11), CD11b (clone M1/70), Ly6g (clone HK1.4), CD4 (clone GK1.5), CD8 (clone 53–6.7), all purchased from eBiosciences (Thermo Fisher Scientific, Waltham, MA, USA), and CD3 (clone 17A2) (BioLegend, San Diego, CA, USA) at 4°C for 30 min. Cells were then fixed using IC fixation buffer (eBiosciences, San Diego, CA, USA). Cytometric acquisition was performed using a BD FACS Canto II flow cytometer and analyzed with FlowJo software (Tree Star, Inc., Ashland, OR, USA).

Author Manuscript Author Manuscript Author Manuscript Author Manuscript

In vivo BBB permeability assay

Mice were injected retroorbitally with 100 μl of 10 kda or 40 kDa dextran-fluorescein in phosphate-buffered saline. At 15 minutes post-injection, mice were perfused with cold PBS. Following PBS-perfusion, the cortex was dissected, homogenized, and centrifuged at 8,000xg for 10 min at room temperature. The supernatant was then isolated and relative fluorescence was measured as described (Bernstein et al., 2019) using a Synergy 2 plate reader (BioTek, Winooski, VT, USA). Fluorescent dye content was calculated using external standards, including collected blood plasma. All data are expressed as relative fluorescent units (RFU) normalized per mg of tissue (Bernstein et al., 2019).

Immunohistochemistry (IHC) analysis

Mice were anesthetized with 5% isoflurane and transcardially perfused with 20 ml cold PBS delivered over a period of 10 minutes, at 3- and 7-days post-stroke. Following perfusion, brains were removed and fixed in 4% formaldehyde solution for 24 h, then embedded in paraffin. Brains were then sectioned coronally on a Leica CM1860 cryostat (Leica Biosystems, Wetzlar, Germany) into 6 μm sections, which were then deparaffinized and washed with PBS, permeabilized with 0.1% Triton X-100 in PBS and blocked for 2 h in 1% BSA, 5% normal donkey serum in PBS/0.1% Triton X-100. Primary antibodies, anti-IBA-1 (1:500, Wako Chemicals, Richmond, VA, USA; Cat# 019–19741 Lot#WDK2121 RRID:AB_839504), and monoclonal anti-NeuN (1:500, Abcam, Cambridge, MA, USA; Cat# ab177487, clone [EPR12763]) was diluted in blocking solution and incubated overnight at 4 °C. Samples were then washed four times in PBS/0.1% Triton X-100 and incubated in secondary antibody diluted in blocking solution for 2 h at room temperature. Brain sections were captured *in toto* at 200X magnification by an Aperio AT2 slide scanner (Leica Biosystems, Wetzlar, Germany) and analyzed via NIS-Elements software (Nikon Instruments, Melville, NY). Regions of interest (ROI) were manually selected to include all structures within a single hemisphere. Within NIS-Elements, GA3 module was used to generate a mask of peroxidase-reactive regions through combination of red-to-blue channel densitometry ratio and elimination of non-microglial nuclei via circularity exclusion filter. A nuclei mask was generated through a similar approach, utilizing sum densitometry of all channels, inclusive circularity filter, and selection of only nuclei which overlapped with only microglial structures. Intensity thresholds for the generation of both masks were manually set by blind observer for each image and inspected to ensure that label omission or extraneous labelling was minimized. Total Iba1-positive area was obtained by dividing peroxidase mask area by total region of interest area, and total length of skeletonized length of skeletonized peroxidase mask was divided by ROI area to normalize. Nuclei count was divided by ROI area to calculate density of microglial cells in each ROI. To examine microglial morphology, peroxidase mask was again generated using a smooth-sharpen preprocessed image. This reduced aberrant classification of extra branch points that can result from process roughness, and bridged small gaps in processes which would otherwise result in false detection of multiple processes. This mask was subsequently skeletonized and filtered for contact with nuclei, yielding whole structure of only the microglia which had nuclei visible in the plane of tissue section. Process length, branch count, process end count, and territory covered were tabulated for each microglia within the ROI, and distance of branch and process end point from nucleus was recorded. Territory covered was determined

Author Manuscript Author Manuscript Author Manuscript Author Manuscript

to be the area of convex hull function applied to whole microglial structure. Mean values of microglial length, territory, branching, and end count were calculated for each ROI and distance distribution of process branch and ending points were compiled for each experimental group using R statistical software (R Foundation for Statistical Computing, Vienna, Austria).

Transendothelial Electrical Resistance (TEER)

BMVEC transfected with miRNA (targeting (let-7g mimic) or non-targeting (scramble) sequences were plated on collagen type I coated 96W20idf electrode arrays (Applied Biophysics, Troy, NY, USA) and were maintained for 72 h to form a monolayer; basal levels of TEER were 800–1500Ω (Ramirez et al., 2013; Rom et al., 2012). A time "zero" was assigned for the experiment with or without TNFα treatment. TEER measurements were performed using the 1600R ECIS System (Applied Biophysics) as described (Rom et al., 2015; Rom et al., 2012; Rom et al., 2013). The results are presented as an average of the resistance values (Ohm, **Ω**) as well as the average percent change from baseline TEER (expressed as average ± SD) from at least three independent experiments consisting of four to six replicates each.

Statistical analysis

Data are expressed as the mean ± SD of experiments conducted multiple times. Data were tested for normality using the Shapiro-Wilk test, and, if data were normally distributed, for multiple group comparisons. Multiple group comparisons were performed by one-way ANOVA with Tukey posthoc test with significance at $p<0.05$ (TEER, FACS, permeability assays, animal experiments). A paired two-tailed Student's test was used to compare before and after effects. Significant differences were considered to be at $p < 0.05$. Statistical analyses were performed utilizing Prism v8 software (GraphPad Software Inc., San Diego, CA, USA).

Results

let-7g* expression is reduced in endothelial cells, in both *in vitro* and *in vivo* models of ischemia/reperfusion (I/R).

Recently, our group has demonstrated that let-7g*, a variant of the let-7 family, was drastically down-regulated during inflammation (Rom et al., 2015). Furthermore, stroke-like conditions have been shown to impact the expression of similar miRNAs from the same let-7 family, such as miR-98 (Bernstein et al., 2019). To evaluate whether expression of let-7g* is particularly affected by ischemia/reperfusion processes, we exposed primary human BMVECs to oxygen and glucose deprivation followed by reperfusion (OGD/R), and then assessed let-7g* expression by qPCR. We determined that BMVECs demonstrated a profound reaction to stroke-like conditions, with a nearly 3.9-fold reduction in let-7g* expression levels following OGD/R ($p < 0.001$) (Fig. 1a). To compare with *in-vivo* models of stroke, we also evaluated let-7g* expression in brain MVs extracted from animals which had undergone tMCAO 24 hr previously. MVs from "stroked" animals showed a similarly lowered by 77% +/− 8%, expression of let-7g* ($p <0.0001$) (Fig. 1b).

Author Manuscript Author Manuscript Author Manuscript Author Manuscript

Overexpression of let-7g* preserves endothelial integrity and limits brain permeability following I/R.

Leakage of the BBB is a critical feature of many forms of neuroinflammation (Shimizu et al., 2013). Particularly following stroke, the vascular endothelial cells lining the BBB become more permeable, allowing the extravasation of toxic blood proteins, cytotoxic leukocytes and lymphocytes into the brain (Bernstein et al., 2019), and worsening inflammatory damage. To investigate whether let-7g* overexpression could potentially produce neuroprotective effects, we utilized *in vitro* and *in vivo* models to measure changes in endothelial barrier integrity following stroke in the presence or absence of elevated let-7g*. By measuring TEER, we assessed BBB integrity by subjecting the BMVECs to OGD/R conditions (a model of I/R) (Bernstein et al., 2019; Rom et al., 2015). While OGD/R lowered the endothelial resistance in all cells, let-7g* overexpression significantly attenuated the degree of decline. In the initial 3 hours following I/R conditions, let-7g*-treated cells displayed a significantly higher TEER value compared with Scr-1-treated cells (Scr-1 = 410 +/− 15 Ω; let-7g = 570 +/− 10 Ω; $p < 0.01$) (Fig 2a). By 5 hr post-OGD/R, TEER levels had returned to baseline levels in the let-7g*-treated cells, a finding which persisted throughout the remainder of the experiment, while Scr-1-treated cells displayed significantly lower TEER, and failed to recover for the entire 24 hr ($p < 0.05$, Fig 2b). This barrier-preserving effect was also observed *in vivo*. We have previously shown that injecting mice with liposome-miRNA complexes of let-7 miRNAs induces a major (20–60 fold) increase in tissue expression by 2 hr after injection, and such overexpression persists for several days (Bernstein et al., 2019; Rom et al., 2015). Mice were subjected to tMCAO and injected with liposome-miRNA complexes as described (Bernstein et al., 2019). 72h following tMCAO, animals were injected with fluorescein-conjugated dextrans of different sizes, followed by intercardiac perfusion with cold PBS. The level of florescence remaining in the brain lysate was used to assess permeability. Fluorescence was significantly attenuated in let-7g*-treated animals, compared with scramble-treated mice (3kd: Control = 260 +/− 14 RFU; scramble = 394 +/− 47 RFU; let-7g* = 292 +/− 31 RFU; $p < 0.005$; Figure 2c) (10kd: Control = 264 +/− 16 RFU; scramble = 474 +/− 61 RFU; let-7g* = 307 +/− 29 RFU; $p < 0.01$; Figure 2d).

Overexpression of let-7g* improves neurological outcomes following stroke

After observing an improvement in BBB tightness, we tested whether overexpression/restoration of let-7g would improve the deficits in neurological function after stroke. In this study, we induced tMCAO in mice, injected them i.v. with let-7g* or non-coding (scramble) miRNA liposomal complex at 2 and 24 hr after tMCAO, following a protocol developed in our laboratory (Bernstein et al., 2019) and tested for neurological outcomes at 72 hr and 7 days post-tMCAO. First, we utilized the corner test to measure hemiparesis, a common feature of many strokes involving the middle cerebral artery. “Stroked” mice usually turn toward the stroke- affected side (right), while non-affected mice have almost a 50–50% left-to-right distribution (DeVries et al., 2001; Zhang et al., 2002). Consistent with the literature, we observed that after tMCAO, mice which had received scramble injections showed 9.5±0.5 out of 10 right-to-left turn distribution (a feature of high impairment), whereas sham animals presented a normal 5±1 out of 10 right-to-left turn distribution. let-7g*-treated mice showed significant improvement (7±1 right-to-left, $p < 0.01$, Fig 3a) in the corner test. At 7

Author Manuscript Author Manuscript Author Manuscript Author Manuscript

days, let-7g* treated mice continued to show this improvement, maintaining a 7±1 right-to-left turn distribution, while scramble miRNA-treated mice had improved to a 8±1 right-to-left distribution vs. the 3 day timepoint, thereby lessening the distinction in the Corner test between the let-7g* and scramble-treated groups at 7 days timepoint (data not shown).

Additionally, we observed significant improvements in locomotor activity, another measure of neurocognitive recovery (Chen et al., 2015; DeVries et al., 2001; Ronca et al., 2015; Winter et al., 2005). tMCAO caused a ~20-fold reduction in locomotor activity in scramble-treated animals at 72 hr timepoint, but only a ~ 40% decrease in activity in let-7g*-treated animals ($p < 0.001$; Fig 3b).

Despite some spontaneous recovery and intensive physical therapy efforts, a significant percent of patients are left with permanent disability, noticed in impairments of motor function, and gait abnormalities, such as decreased velocity, pace, stride length, and extended swing phase on the affected side, in addition to reduced ambulation and balance impairments (Parkkinen et al., 2013). With this information in mind, we decided to assess whether over-expression of let-7g* would improve gait functions after tMCAO. Indeed, we observed significant improvement in the gait of mice who had received let-7g* after stroke. Gait, or walking pattern, is a measure of both motor deficits (foot stride length) and of preservation of overall neurocognitive deficits (stride pattern and footprint) (Chen et al., 2019; Hetze et al., 2012). Three days post stroke, we observed that treatment with let-7g* preserved the normal distance between toes in the rear limb ($p < 0.01$; Fig 4a and 4e). In addition, the average stride length of the front limb ($p < 0.05$; Fig 4b) and the rear limb ($p < 0.005$; Fig 4d) of the affected side were significantly improved by let-7g treatment, although no difference was observed in toe spread of the front paw ($p > 0.05$; Fig 4c). Further, such improvements persisted at 7 days post-stroke. let-7g* treated mice continued significant recovery in front and rear stride length ($p < 0.05$; Fig 4b and 4d) compared with scramble-treated mice. Recovery to rear paw spread was also observed, although it was not statistically significant ($p = 0.0511$; Fig 4e). These results suggest that treatments which increase let-7g* expression may improve outcomes if given promptly after the onset of a stroke.

let-7g* overexpression mitigates neuroinflammation after stroke.

Endothelial dysfunction, a critical feature of stroke (Bernstein et al., 2019; Zhang, 2008), can trigger inflammatory processes arising from within the brain (microglia) (Faraco et al., 2017) as well as from the peripheral immune system (leukocytes, lymphocytes, neutrophils) (Jimenez et al., 2008). After observing some preservation of BBB integrity, as well as improved clinical outcomes, we next assessed cellular measures of inflammation arising from both sides of the BBB. To measure within-brain inflammation, we injected animals i.v. with let-7g* or scramble following tMCAO, and perfused them 72 hr later. We then evaluated microglial number and activation within the infarcted hemisphere. We observed that let-7g* significantly reduced the number of Iba1+ cells within the infarcted hemisphere ($p < 0.05$; Fig. 5b) along with their overall distribution ($p < 0.01$; Fig 5c). Additionally, overexpression of let-7g* also reduced the activation state of microglia within area, both in terms of overall size (Fig 5a) and in the number of processes ($p < 0.05$; Fig 5a and 5e).

Author Manuscript Author Manuscript Author Manuscript Author Manuscript

While not statistically significant, there was a strong trend toward a smaller overall area per Iba1+ cell as well (Fig 5d). At 1-week post-stroke, let-7g* treated animals continued to show improvement in total IBA+ cell activation, total affected area, and total processes, compared with scramble-treated animals (data not shown). In addition, inflammatory responses arising from the peripheral blood were significantly contained by overexpression of let-7g*. At 72 hr after stroke, brain-infiltrating leukocytes (BILs) were isolated from mouse brains and stained with tagged antibodies in order to count cell types through FACS. With all gating measures set at the same level (Fig 6a), we observed significant reductions in immune cell infiltration into the brain following let-7g* treatment. The total number of CD45+ BILs was reduced by more than 50% ($p < 0.05$; Fig 6b), as was the number of overall CD3+ T cells ($p < 0.005$; Fig 6c), CD4+ helper T cells ($p < 0.05$; Fig 6d), and neutrophils ($p < 0.05$; Fig 6F). Curiously, the percentage of CD8+ cytotoxic T cells was not significantly increased following stroke, nor decreased following let-7g* overexpression (Fig 6e). These results point to the importance of an intact brain endothelium in limiting post-stroke inflammation from both sides of the BBB, and postulate a significant role for let-7g* in mediating these processes.

let-7g* overexpression provides neuroprotection after stroke.

After observing that let-7g* overexpression improves neurocognitive improvements, increases BBB integrity, and reduces brain inflammation, we sought to determine whether stroke-induced neuron loss was also reduced and whether the effects we observed were truly neuroprotective. To address this question, we sacrificed animals 72 hr or 7 days after stroke, and stained brain section regions for NeuN, a neuronal marker for intact nuclei. In the infarcted brain hemisphere of scramble-treated animals, we observed a loss of nearly 50% and 64% of all neurons at 72 hr and 7 days post stroke, respectively ($p < 0.005$, Fig 7a and 7b), a finding which is similar to that published in the literature (Emmrich et al., 2015). However, this decrease was strongly attenuated by let-7g* overexpression, with treated animals showing 25%±8% and 20%±4% loss of neurons at 72 hr and 7 days post-stroke, respectively, representing a preservation of more than half of the cells lost in scramble-treated animals ($p<0.05$, Fig 7b), as well as a more preserved cortical structure (Fig 7a). Taken together, these data show that let-7g* expression is strongly neuroprotective, and restoring levels to at or near pre-stroke levels can significantly prevent much of the damage following stroke, and lead to better clinical outcomes.

Discussion

In the current experiments, we have identified a critical regulator of the brain endothelial response to stroke. To our knowledge, we are the first research group to illustrate the role of let-7g* in modulating the inflammatory and immune responses following ischemic events. We have also shown a correlative link between physiological alterations outside of the BBB, and changes to cellular morphology within. First, we demonstrate that let-7g* miRNA is significantly downregulated following stroke-like conditions in both *in vitro* and *in vivo* models of ischemia/reperfusion, a finding which is corroborated by a growing number of studies describing the potential role of let-7 miRs in modulating neuroinflammation (Bernstein et al., 2019; Cho et al., 2015; Makino et al., 2013; Rom et al., 2015). Since let-7's

Author Manuscript Author Manuscript Author Manuscript Author Manuscript

miRNAs in general, and let-7g*, particularly, has been shown to bind to many secondary messengers associated with cytokine release (Bernstein et al., 2019; Pan et al., 2011; Rom et al., 2015), we sought to determine whether restoring its expression after an ischemic event could limit inflammatory responses, and ultimately improve neurological recovery. We determined that when given within hours of a stroke, let-7g* is capable of ameliorating many of its more destructive features. Such beneficial effects include a preservation of neural tissue, reduced BBB permeability, an attenuated immune response, and greater behavioral outcome measures.

Gait, or walking pattern, is critically affected after neurological events such as stroke or TBI, and is a measure of both motor deficits (foot stride length) and of preservation of overall neurocognitive deficits (stride pattern and footprint) (Chen et al., 2019; Hetze et al., 2012). Gait is not only an indicator of lower extremity motor function, but also reflects on cognitive function, specifically executive function (Wang et al., 2008). In spite of some natural recovery and thorough physical therapy efforts, one quarter (25%) of stroke survivors are left with everlasting disability, observed in impairments of motor function, and gait abnormalities, such as decreased velocity, pace, stride length, and extended swing phase on the affected side, in addition to reduced ambulation and balance impairment (Parkkinen et al., 2013). Our results indicate that let-7g* miRNA improves gait in post-stroke mice and denotes the importance of let-7g* as a critical element of the ischemic cascade as a potential pharmacological target for future therapies for treating or preventing post-ischemic stroke disabilities.

let-7 is of particular importance due in part to its influence on brain endothelial cells. These cells are a main component of the BBB and their injury represents one of the earliest and most critical measures of neuroinflammation (Ao et al., 2018; Li et al., 2018b); indeed, many elements of immune cell activation (Lopes Pinheiro et al., 2016), adhesion (Ludewig et al., 2019), and cytokine production (Verma et al., 2006) can arise from and ultimately worsen endothelial dysfunction. We have shown that restored expression of let-7g*, in addition to that of miR-98, another let-7 miR (Bernstein et al., 2019; Rom et al., 2015), can help preserve the endothelial component of the BBB, and break the toxic cycle of cell dysfunction and infiltration of cytotoxic cells from across BBB.

Critically, such neuroprotective effects of let-7g* are likely not confined to stroke. miRs from the let-7 family directly reduce the expression of certain cytokines, such as MCP-1/CCL2 and CCL5 (Rom et al., 2015), which are involved in the disease process of BBB inflammation that occurs during traumatic brain injury (Albert et al., 2017; Lumpkins et al., 2008), diabetes (Lee et al., 2019; Teler et al., 2017; Zhang, 2008) and multiple forms of encephalitis (Chowdhury and Khan, 2017). While there are many causes of neuroinflammation, ranging from genetic abnormalities (Krementsov et al., 2018) to bacterial infection (Singer et al., 2018), many of them involve increased levels of these particular cytokines, which can cause leukocyte adhesion (Schober, 2008) and rearrangement of tight junction proteins on endothelial cells (Stamatovic et al., 2005), leading to BBB compromise. BBB disruption, upregulation of cell adhesion molecules, and activation of resident microglia develop the post-stroke neuro-immune interactions. Within 24 hr of stroke onset, adaptive immune cells, including T cells, are detected in the brain

Author Manuscript Author Manuscript Author Manuscript Author Manuscript

(Herz et al., 2015; Jin et al., 2010). Migration of these cells peaks around 3–4 days post-stroke, and helper $CD4^+$ and cytotoxic $CD8^+$ T cells persist in the perilesional tissue for weeks after injury, implicating this leukocyte subset in long-term recovery (Gelderblom et al., 2009; Poinsatte et al., 2019; Xie et al., 2018). Neutrophils are the primary cells in the blood to respond after ischemic stroke, contributing to disruption of the BBB, brain edema and injury. Neutrophils also are involved in the major processes that cause ischemic stroke, thrombosis and atherosclerosis (Jin et al., 2010). These disruptive inputs are mediated by factors released from neutrophils including reactive oxygen species (ROS) (superoxide, hypochlorous acid), proteases (matrix metalloproteinases, elastase, cathepsin G, proteinase 3), cytokines (IL-1β, IL-6, IL-8, tumor necrosis factor alpha (TNF-α)), and chemokines (CCL2, CCL3, CCL5) (Jickling et al., 2015). Our results show that let-7g* significantly reduced the presence of BILs, especially neutrophils and CD4+ T cells. Zhang and colleagues, have recently shown that inhibition of CD4 T cells reduces stroke-induced infarction (Zhang et al., 2018). By slowing this process, let-7g* could have significant potential for ameliorating the effects of many different neuroinflammatory diseases, including chronic conditions with a much longer “treatment window” than stroke. Remarkably, let-7g* overexpression impacted neutrophil migration, as well as infiltration of T cells, but had no significant effect on the infiltration of monocytes, cells which also reach peak levels at 24–72 hr post-infarct (Shi and Pamer, 2011). As monocytes are precursors to macrophages, this finding suggests that let-7g* may be ameliorating inflammation by limiting the activation of T cells, and of endogenous microglia within the CNS. Interestingly, another let-7 miRNA, miR-98, has been shown the ability to significantly decrease infiltration of monocytes at a 3 day timepoint (Bernstein et al., 2019). Since these miRNAs are slightly different in their sequence, they might have distinctive targets and therefore diverse effects, which requires future studies.

Another important attribute of let-7g* is that it is endogenously expressed within endothelial cells (Rom et al., 2015), which lie on the luminal side of the BBB. Therefore, it is a clinically accessible target for potential stroke pharmacotherapies. By focusing on cells comprising the proximal blood vessels, our approach offers the promise of high bioavailability and ease in reaching the target areas. Without the need to cross the BBB, molecules such as let-7g* will have high bioavailability to their intended target cells, and can begin working immediately. Indeed, we observe significant protective effects when administering let-7g* within 2 hr of ischemic event, making it highly relevant for stroke therapies.

Although let-7g* overexpression produces effects almost immediately, the neuroprotective impact extends for many hours after ischemia. As demonstrated in Figure 2a–b, a single treatment with let-7g* induces stronger barrier integrity after I/R, and continues throughout the entire experimental period, ultimately restoring barrier tightness (TEER) to baseline levels. This long duration of effect suggests a continuous role in mediating the cellular response to hypoxic stress, as well as an extended window in which it may be targeted for therapeutic effect. By improving BBB tightness and limiting immune cell recruitment, let-7g* overexpression slows the rate of tissue death and improves functional outcomes after an ischemic stroke. This is evidenced by the significant improvements in all behavior tests

Author Manuscript Author Manuscript Author Manuscript Author Manuscript

and less injury to brain tissue at 72hr, and these improvements persisted through 1 week after the stroke (Figures 3, 4 and 7).

Finally, the rapid-onset, yet extended-duration period of neuroprotection conferred by restored let-7g* expression offers promise for *preventing* future strokes, in addition to managing the symptoms following an ischemic attack. During most surgical procedures, there is an increased risk of perioperative stroke, due to bleeding, and due to the possibility of tissue debris entering the bloodstream and promoting a clot formation. The risk can run to over 10% for high-risk cardiac surgery procedures (Ko, 2018) and, in susceptible individuals, can cause mortality rates which approach 60% (Sharifpour et al., 2013; Vlisides and Mashour, 2016). As most vascular blockages often go undetected until becoming complete, their management could be conferred through agents which increase let-7g* expression, thereby leading to improved clinical outcomes for patients undergoing surgery, and do much to make surgeries safer.

Such enhancements might not be necessarily to be restricted to the brain; let-7 miRs are present in most tissues and cell types in the body (Bernstein et al., 2019; Chen et al., 2011; Cho et al., 2015; Gan et al., 2019; Jiang et al., 2017; Liu et al., 2011; Ludwig et al., 2016; Roush and Slack, 2008; Tolonen et al., 2014; Wang et al., 2012). Hence, it is possible that some of the let-7 extracted from the MVs could have been formed by mural cells such as pericytes, in addition to BMVECs. Endothelial to pericyte ratios in normal tissues vary between 1:1 and 10:1, while pericyte coverage of the endothelial abluminal surface ranges between 70% and 10%, with the highest ratio in retina vessels (Armulik et al., 2011; Armulik et al., 2010; Geevarghese and Herman, 2014; Park et al., 2019). Furthermore, ischemia/reperfusion conditions reproduced by OGD/R resulting in changes to let-7g* expression (Figure 1a) were attributable only to expression occurring within BMVECs themselves. Hence, it is possible that mural cells contribute to the overall expression of let-7g*, but endothelial cells appear to be responsible for a significant proportion of its expression within the microvasculature. Generally, let-7’ miRs are downregulated during inflammatory insults, and restoration of expression can lead to preservation of cellular function across a variety of conditions (Bernstein et al., 2019; Liao et al., 2014; Liu et al., 2017; Rom et al., 2015).

Due to the systemic treatment of the liposomal-let-7g* complex, it is probable that other organs/tissues were also targeted. We identified that let-7g* expression was vigorous within the brain microvasculature, to a slighter degree within the brain itself, and some extent in other organs. Based on our current data and results from our previous work (Bernstein et al., 2019; Rom et al., 2015), we believe that the beneficial effects of let-7 on cerebral ischemia are due to direct impact on the microvasculature. Recently, we demonstrated that let-7 miRs, miR-98 and let-7g*, are directly target expression of proinflammatory cytokines, CCL2 and CCL5 (Rom et al., 2015). Both above-mentioned cytokines are known to enable acute inflammatory responses and promote leukocyte adhesion to and migration across the BBB (Schober, 2008), as well as decreasing BBB tightness by changing small Rho GTPase activation, triggering actin cytoskeleton rearrangements and provoking redistribution of TJ proteins, ZO-1, ZO-2, occludin and claudin-5 (Stamatovic et al., 2005). Reasonably, we

Author Manuscript Author Manuscript Author Manuscript Author Manuscript

think that most of the stroke protective effects are coming from endothelial cells transfected with let-7g*.

Taken together, let-7g* overexpression represents a novel opportunity in treating ischemic stroke, due to its combination of rapid onset and long window of clinical effects. In addition, let-7g* offers the potential for ameliorating the effects of other forms of neuroinflammation, due to the ubiquity of the cellular signaling mechanisms which it acts upon. After ischemic or traumatic events, the cerebral vasculature is often significantly damaged and this damage can undermine the integrity of the BBB for weeks after injury (Ju et al., 2018; Sulhan et al., 2020). Hence, molecules directly targeting the BBB (such as let-7g*) may have a therapeutic window, which extends far beyond the 3–6 hr timeframe often recommended for tPA. These attributes offer great promise for future clinical utility.

This study expands upon previous work which identified let-7 miRs as targets of neuroinflammation (Rom et al., 2015) and quantifies this utility in the context of stroke (Bernstein et al., 2019). We have since determined several important mechanisms through which let-7 miRs can promote neuroprotection, through cytokine signaling and immune cell activation, and characterized the timeline of such effects to a week following the ischemic insult. While research on let-7 miRs is still growing, studies such as this lay an important foundation for developing treatments for stroke and other neuroinflammatory diseases, and provide a greater understanding of the pathophysiology of one of the world's most devastating diseases.

Acknowledgments

This work was supported in part by NIH research grants R01NS101135 (SR), R01AA015913 (YP) and R01MH115786 (YP).

References:

Ahnstedt H, Sweet J, Cruden P, Bishop N, Cipolla MJ, 2016 Effects of Early Post-Ischemic Reperfusion and tPA on Cerebrovascular Function and Nitrosative Stress in Female Rats. Translational stroke research 7, 228–238. [PubMed: 27125535]

Albert V, Subramanian A, Agrawal D, Bhoi SK, Pallavi P, Mukhopadhayay AK, 2017 RANTES levels in peripheral blood, CSF and contused brain tissue as a marker for outcome in traumatic brain injury (TBI) patients. BMC research notes 10, 139. [PubMed: 28340601]

Ao LY, Yan YY, Zhou L, Li CY, Li WT, Fang WR, Li YM, 2018 Immune Cells After Ischemic Stroke Onset: Roles, Migration, and Target Intervention. Journal of molecular neuroscience : MN 66, 342–355. [PubMed: 30276612]

Armulik A, Genove G, Betsholtz C, 2011 Pericytes: developmental, physiological, and pathological perspectives, problems, and promises. Dev Cell 21, 193–215. [PubMed: 21839917]

Armulik A, Genove G, Mae M, Nisancioglu MH, Wallgard E, Niaudet C, He L, Norlin J, Lindblom P, Strittmatter K, Johansson BR, Betsholtz C, 2010 Pericytes regulate the blood-brain barrier. Nature 468, 557–561. [PubMed: 20944627]

Balkaya M, Kröber JM, Rex A, Endres M, 2013 Assessing post-stroke behavior in mouse models of focal ischemia. J Cereb Blood Flow Metab 33, 330–338. [PubMed: 23232947]

Bartel DP, 2004 MicroRNAs: genomics, biogenesis, mechanism, and function. Cell 116, 281–297. [PubMed: 14744438]

Bernstein DL, Zuluaga-Ramirez V, Gajghate S, Reichenbach NL, Polyak B, Persidsky Y, Rom S, 2019 miR-98 reduces endothelial dysfunction by protecting blood-brain barrier (BBB) and improves

Author Manuscript Author Manuscript Author Manuscript Author Manuscript

neurological outcomes in mouse ischemia/reperfusion stroke model. J Cereb Blood Flow Metab, 271678×19882264.

Beurel E, 2011 Regulation by glycogen synthase kinase-3 of inflammation and T cells in CNS diseases. Front Mol Neurosci 4, 18. [PubMed: 21941466]

Brennan E, Wang B, McClelland A, Mohan M, Marai M, Beuscart O, Derouiche S, Gray S, Pickering R, Tikellis C, de Gaetano M, Barry M, Belton O, Ali-Shah ST, Guiry P, Jandeleit-Dahm KAM, Cooper ME, Godson C, Kantharidis P, 2017 Protective Effect of let-7 miRNA Family in Regulating Inflammation in Diabetes-Associated Atherosclerosis. Diabetes 66, 2266–2277. [PubMed: 28487436]

Chen KC, Hsieh IC, Hsi E, Wang YS, Dai CY, Chou WW, Juo SH, 2011 Negative feedback regulation between microRNA let-7g and the oxLDL receptor LOX-1. J Cell Sci 124, 4115–4124. [PubMed: 22135361]

Chen M, Lyu H, Li T, Su XW, Leung CK, Xiong MZQ, Poon WS, Cai YF, Lu G, Chan WY, Wang LX, 2019 Study of the association between gait variability and gene expressions in a mouse model of transient focal ischemic stroke. The International journal of neuroscience, 1–19.

Chen QF, Liu YY, Pan CS, Fan JY, Yan L, Hu BH, Chang X, Li Q, Han JY, 2018 Angioedema and Hemorrhage After 4.5-Hour tPA (Tissue-Type Plasminogen Activator) Thrombolysis Ameliorated by T541 via Restoring Brain Microvascular Integrity. Stroke 49, 2211–2219. [PubMed: 30354988]

Chen Y, Zhu W, Zhang W, Libal N, Murphy SJ, Offner H, Alkayed NJ, 2015 A novel mouse model of thromboembolic stroke. J Neurosci Methods 256, 203–211. [PubMed: 26386284]

Cho KJ, Song J, Oh Y, Lee JE, 2015 MicroRNA-Let-7a regulates the function of microglia in inflammation. Mol Cell Neurosci 68, 167–176. [PubMed: 26221772]

Chowdhury P, Khan SA, 2017 Significance of CCL2, CCL5 and CCR2 polymorphisms for adverse prognosis of Japanese encephalitis from an endemic population of India. Scientific reports 7, 13716. [PubMed: 29057937]

Chun HB, Scott M, Niessen S, Hoover H, Baird A, Yates J 3rd, Torbett BE, Eliceiri BP, 2011 The proteome of mouse brain microvessel membranes and basal lamina. J Cereb Blood Flow Metab 31, 2267–2281. [PubMed: 21792245]

Conductier G, Blondeau N, Guyon A, Nahon JL, Rovere C, 2010 The role of monocyte chemoattractant protein MCP1/CCL2 in neuroinflammatory diseases. J Neuroimmunol 224, 93–100. [PubMed: 20681057]

de Oliveira S, Rosowski EE, Huttenlocher A, 2016 Neutrophil migration in infection and wound repair: going forward in reverse. Nat Rev Immunol 16, 378–391. [PubMed: 27231052]

del Zoppo GJ, 2009 Inflammation and the neurovascular unit in the setting of focal cerebral ischemia. Neuroscience 158, 972–982. [PubMed: 18824084]

del Zoppo GJ, von Kummer R, Hamann GF, 1998 Ischaemic damage of brain microvessels: inherent risks for thrombolytic treatment in stroke. J Neurol Neurosurg Psychiatry 65, 1–9. [PubMed: 9667553]

DeVries AC, Nelson RJ, Traystman RJ, Hurn PD, 2001 Cognitive and behavioral assessment in experimental stroke research: will it prove useful? Neurosci Biobehav Rev 25, 325–342. [PubMed: 11445138]

Eder PS, DeVine RJ, Dagle JM, Walder JA, 1991 Substrate specificity and kinetics of degradation of antisense oligonucleotides by a 3’ exonuclease in plasma. Antisense research and development 1, 141–151. [PubMed: 1841656]

Emmrich JV, Ejaz S, Neher JJ, Williamson DJ, Baron JC, 2015 Regional distribution of selective neuronal loss and microglial activation across the MCA territory after transient focal ischemia: quantitative versus semiquantitative systematic immunohistochemical assessment. J Cereb Blood Flow Metab 35, 20–27. [PubMed: 25352044]

Engel O, Kolodziej S, Dirnagl U, Prinz V, 2011 Modeling stroke in mice - middle cerebral artery occlusion with the filament model. Journal of visualized experiments : JoVE.

Faraco G, Park L, Anrather J, Iadecola C, 2017 Brain perivascular macrophages: characterization and functional roles in health and disease. Journal of molecular medicine (Berlin, Germany) 95, 1143–1152.

Author Manuscript Author Manuscript Author Manuscript Author Manuscript

Feng Y, Liao S, Wei C, Jia D, Wood K, Liu Q, Wang X, Shi FD, Jin WN, 2017 Infiltration and persistence of lymphocytes during late-stage cerebral ischemia in middle cerebral artery occlusion and photothrombotic stroke models. J Neuroinflammation 14, 248. [PubMed: 29246244]

Gan H, Lin L, Hu N, Yang Y, Gao Y, Pei Y, Chen K, Sun B, 2019 Aspirin ameliorates lung cancer by targeting the miR-98/WNT1 axis. Thoracic cancer 10, 744–750. [PubMed: 30756509]

Geevarghese A, Herman IM, 2014 Pericyte-endothelial crosstalk: implications and opportunities for advanced cellular therapies. Transl Res 163, 296–306. [PubMed: 24530608]

Gelderblom M, Leypoldt F, Steinbach K, Behrens D, Choe CU, Siler DA, Arumugam TV, Orthey E, Gerloff C, Tolosa E, Magnus T, 2009 Temporal and spatial dynamics of cerebral immune cell accumulation in stroke. Stroke 40, 1849–1857. [PubMed: 19265055]

Herz J, Sabellek P, Lane TE, Gunzer M, Hermann DM, Doeppner TR, 2015 Role of Neutrophils in Exacerbation of Brain Injury After Focal Cerebral Ischemia in Hyperlipidemic Mice. Stroke 46, 2916–2925. [PubMed: 26337969]

Hetze S, Romer C, Teufelhart C, Meisel A, Engel O, 2012 Gait analysis as a method for assessing neurological outcome in a mouse model of stroke. J Neurosci Methods 206, 7–14. [PubMed: 22343052]

Inserra MM, Bloch DA, Terris DJ, 1998 Functional indices for sciatic, peroneal, and posterior tibial nerve lesions in the mouse. Microsurgery 18, 119–124. [PubMed: 9674927]

Jiang J, Chen Z, Yang Y, Yan J, Jiang H, 2017 Sevoflurane downregulates IGF1 via microRNA98. Molecular medicine reports 15, 1863–1868. [PubMed: 28260068]

Jiang N, Zhang X, Zheng X, Chen D, Siu K, Wang H, Ichim TE, Quan D, McAlister V, Chen G, Min WP, 2012 A novel in vivo siRNA delivery system specifically targeting liver cells for protection of ConA-induced fulminant hepatitis. PLoS One 7, e44138. [PubMed: 22970170]

Jickling GC, Liu D, Ander BP, Stamova B, Zhan X, Sharp FR, 2015 Targeting neutrophils in ischemic stroke: translational insights from experimental studies. J Cereb Blood Flow Metab 35, 888–901. [PubMed: 25806703]

Jimenez JJ, Jy W, Mauro LM, Horstman LL, Fontana V, Ahn YS, 2008 Transendothelial migration of leukocytes is promoted by plasma from a subgroup of immune thrombocytopenic purpura patients with small-vessel ischemic brain disease. American journal of hematology 83, 206–211. [PubMed: 17876771]

Jin R, Yang G, Li G, 2010 Inflammatory mechanisms in ischemic stroke: role of inflammatory cells. J Leukoc Biol 87, 779–789. [PubMed: 20130219]

Jin YH, Kim BS, 2015 Isolation of CNS-infiltrating and Resident Microglial Cells. Bio Protoc 5.

Ju F, Ran Y, Zhu L, Cheng X, Gao H, Xi X, Yang Z, Zhang S, 2018 Increased BBB Permeability Enhances Activation of Microglia and Exacerbates Loss of Dendritic Spines After Transient Global Cerebral Ischemia. Front Cell Neurosci 12, 236. [PubMed: 30123113]

Kepplinger J, Barlinn K, Deckert S, Scheibe M, Bodechtel U, Schmitt J, 2016 Safety and efficacy of thrombolysis in telestroke: A systematic review and meta-analysis. Neurology 87, 1344–1351. [PubMed: 27566746]

Knecht T, Borlongan C, Dela Pena I, 2018 Combination therapy for ischemic stroke: Novel approaches to lengthen therapeutic window of tissue plasminogen activator. Brain circulation 4, 99–108. [PubMed: 30450415]

Ko SB, 2018 Perioperative stroke: pathophysiology and management. Korean journal of anesthesiology 71, 3–11. [PubMed: 29441169]

Krementsov DN, Asarian L, Fang Q, McGill MM, Teuscher C, 2018 Sex-Specific Gene-by-Vitamin D Interactions Regulate Susceptibility to Central Nervous System Autoimmunity. Front Immunol 9, 1622. [PubMed: 30065723]

Ku JM, Taher M, Chin KY, Grace M, McIntyre P, Miller AA, 2016 Characterisation of a mouse cerebral microvascular endothelial cell line (bEnd.3) after oxygen glucose deprivation and reoxygenation. Clin Exp Pharmacol Physiol.

Larson SD, Jackson LN, Chen LA, Rychahou PG, Evers BM, 2007 Effectiveness of siRNA uptake in target tissues by various delivery methods. Surgery 142, 262–269. [PubMed: 17689694]

Author Manuscript Author Manuscript Author Manuscript Author Manuscript

Lee CP, Nithiyanantham S, Hsu HT, Yeh KT, Kuo TM, Ko YC, 2019 ALPK1 regulates streptozotocin-induced nephropathy through CCL2 and CCL5 expressions. J Cell Mol Med 23, 7699–7708. [PubMed: 31557402]

Li S, Chen L, Zhou X, Li J, Liu J, 2019 miRNA-223–3p and let-7b-3p as potential blood biomarkers associated with the ischemic penumbra in rats. Acta neurobiologiae experimentalis 79, 205–216. [PubMed: 31342956]

Li S, Francisco GE, Zhou P, 2018a Post-stroke Hemiplegic Gait: New Perspective and Insights. Front Physiol 9, 1021. [PubMed: 30127749]

Li W, Pan R, Qi Z, Liu KJ, 2018b Current progress in searching for clinically useful biomarkers of blood-brain barrier damage following cerebral ischemia. Brain circulation 4, 145–152. [PubMed: 30693340]

Liao YC, Wang YS, Guo YC, Lin WL, Chang MH, Juo SH, 2014 Let-7g improves multiple endothelial functions through targeting transforming growth factor-beta and SIRT-1 signaling. Journal of the American College of Cardiology 63, 1685–1694. [PubMed: 24291274]

Liu M, Tao G, Liu Q, Liu K, Yang X, 2017 MicroRNA let-7g alleviates atherosclerosis via the targeting of LOX-1 in vitro and in vivo. Int J Mol Med 40, 57–64. [PubMed: 28535009]

Liu Y, Chen Q, Song Y, Lai L, Wang J, Yu H, Cao X, Wang Q, 2011 MicroRNA-98 negatively regulates IL-10 production and endotoxin tolerance in macrophages after LPS stimulation. FEBS Lett 585, 1963–1968. [PubMed: 21609717]

Lopes Pinheiro MA, Kooij G, Mizee MR, Kamermans A, Enzmann G, Lyck R, Schwaninger M, Engelhardt B, de Vries HE, 2016 Immune cell trafficking across the barriers of the central nervous system in multiple sclerosis and stroke. Biochim Biophys Acta 1862, 461–471. [PubMed: 26527183]

Ludewig P, Winneberger J, Magnus T, 2019 The cerebral endothelial cell as a key regulator of inflammatory processes in sterile inflammation. J Neuroimmunol 326, 38–44. [PubMed: 30472304]

Ludwig N, Leidinger P, Becker K, Backes C, Fehlmann T, Pallasch C, Rheinheimer S, Meder B, Stahler C, Meese E, Keller A, 2016 Distribution of miRNA expression across human tissues. Nucleic Acids Res 44, 3865–3877. [PubMed: 26921406]

Lumpkins K, Bochicchio GV, Zagol B, Ulloa K, Simard JM, Schaub S, Meyer W, Scalea T, 2008 Plasma levels of the beta chemokine regulated upon activation, normal T cell expressed, and secreted (RANTES) correlate with severe brain injury. J Trauma 64, 358–361. [PubMed: 18301198]

Makino K, Jinnin M, Hirano A, Yamane K, Eto M, Kusano T, Honda N, Kajihara I, Makino T, Sakai K, Masuguchi S, Fukushima S, Ihn H, 2013 The downregulation of microRNA let-7a contributes to the excessive expression of type I collagen in systemic and localized scleroderma. J Immunol 190, 3905–3915. [PubMed: 23509348]

Meresse S, Dehouck MP, Delorme P, Bensaid M, Tauber JP, Delbart C, Fruchart JC, Cecchelli R, 1989 Bovine brain endothelial cells express tight junctions and monoamine oxidase activity in long-term culture. J Neurochem 53, 1363–1371. [PubMed: 2571674]

Minami M, 2011 [Neuro-glio-vascular interaction in ischemic brains]. Yakugaku zasshi : Journal of the Pharmaceutical Society of Japan 131, 539–544. [PubMed: 21467793]

Nour M, Scalzo F, Liebeskind DS, 2013 Ischemia-reperfusion injury in stroke. Interventional neurology 1, 185–199. [PubMed: 25187778]

Pan W, Stone KP, Hsuchou H, Manda VK, Zhang Y, Kastin AJ, 2011 Cytokine signaling modulates blood-brain barrier function. Curr Pharm Des 17, 3729–3740. [PubMed: 21834767]

Park TE, Mustafaoglu N, Herland A, Hasselkus R, Mannix R, FitzGerald EA, Prantil-Baun R, Watters A, Henry O, Benz M, Sanchez H, McCrea HJ, Goumnerova LC, Song HW, Palecek SP, Shusta E, Ingber DE, 2019 Hypoxia-enhanced Blood-Brain Barrier Chip recapitulates human barrier function and shuttling of drugs and antibodies. Nat Commun 10, 2621. [PubMed: 31197168]

Parkkinen S, Ortega FJ, Kuptsova K, Huttunen J, Tarkka I, Jolkkonen J, 2013 Gait impairment in a rat model of focal cerebral ischemia. Stroke Res Treat 2013, 410972. [PubMed: 23533959]

Poinsatte K, Betz D, Torres VO, Ajay AD, Mirza S, Selvaraj UM, Plautz EJ, Kong X, Gokhale S, Meeks JP, Ramirez DMO, Goldberg MP, Stowe AM, 2019 Visualization and Quantification of

Author Manuscript Author Manuscript Author Manuscript Author Manuscript

Post-stroke Neural Connectivity and Neuroinflammation Using Serial Two-Photon Tomography in the Whole Mouse Brain. Frontiers in neuroscience 13.

Posada-Duque RA, Barreto GE, Cardona-Gomez GP, 2014 Protection after stroke: cellular effectors of neurovascular unit integrity. Front Cell Neurosci 8, 231. [PubMed: 25177270]

Quinn SR, O'Neill LA, 2014 The role of microRNAs in the control and mechanism of action of IL-10. Curr Top Microbiol Immunol 380, 145–155. [PubMed: 25004817]

Ramirez SH, Fan S, Dykstra H, Rom S, Mercer A, Reichenbach NL, Gofman L, Persidsky Y, 2013 Inhibition of Glycogen Synthase Kinase 3beta Promotes Tight Junction Stability in Brain Endothelial Cells by Half-Life Extension of Occludin and Claudin-5. PLoS One 8, e55972. [PubMed: 23418486]

Rom S, Dykstra H, Zuluaga-Ramirez V, Reichenbach NL, Persidsky Y, 2015 miR-98 and let-7g* protect the blood-brain barrier under neuroinflammatory conditions. J Cereb Blood Flow Metab 35, 1957–1965. [PubMed: 26126865]

Rom S, Fan S, Reichenbach N, Dykstra H, Ramirez SH, Persidsky Y, 2012 Glycogen synthase kinase 3beta inhibition prevents monocyte migration across brain endothelial cells via Rac1-GTPase suppression and down-regulation of active integrin conformation. Am J Pathol 181, 1414–1425. [PubMed: 22863953]

Rom S, Zuluaga-Ramirez V, Dykstra H, Reichenbach NL, Pacher P, Persidsky Y, 2013 Selective activation of cannabinoid receptor 2 in leukocytes suppresses their engagement of the brain endothelium and protects the blood-brain barrier. Am J Pathol 183, 1548–1558. [PubMed: 24055259]

Ronca RD, Myers AM, Ganea D, Tuma RF, Walker EA, Ward SJ, 2015 A selective cannabinoid CB2 agonist attenuates damage and improves memory retention following stroke in mice. Life Sci 138, 72–77. [PubMed: 26032254]

Roush S, Slack FJ, 2008 The let-7 family of microRNAs. Trends Cell Biol 18, 505–516. [PubMed: 18774294]

Ryg-Cornejo V, Ioannidis LJ, Hansen DS, 2013 Isolation and analysis of brain-sequestered leukocytes from Plasmodium berghei ANKA-infected mice. Journal of visualized experiments : JoVE.

Schober A, 2008 Chemokines in vascular dysfunction and remodeling. Arterioscler Thromb Vasc Biol 28, 1950–1959. [PubMed: 18818421]

Sharifpour M, Moore LE, Shanks AM, Didier TJ, Kheterpal S, Mashour GA, 2013 Incidence, predictors, and outcomes of perioperative stroke in noncarotid major vascular surgery. Anesthesia and analgesia 116, 424–434. [PubMed: 23115255]

Shi C, Pamer EG, 2011 Monocyte recruitment during infection and inflammation. Nat Rev Immunol 11, 762–774. [PubMed: 21984070]

Shimizu F, Sano Y, Tominaga O, Maeda T, Abe MA, Kanda T, 2013 Advanced glycation end-products disrupt the blood-brain barrier by stimulating the release of transforming growth factor-beta by pericytes and vascular endothelial growth factor and matrix metalloproteinase-2 by endothelial cells in vitro. Neurobiol Aging 34, 1902–1912. [PubMed: 23428182]

Singer BH, Dickson RP, Denstaedt SJ, Newstead MW, Kim K, Falkowski NR, Erb-Downward JR, Schmidt TM, Huffnagle GB, Standiford TJ, 2018 Bacterial Dissemination to the Brain in Sepsis. Am J Respir Crit Care Med 197, 747–756. [PubMed: 29232157]

Stamatovic SM, Shakui P, Keep RF, Moore BB, Kunkel SL, Van Rooijen N, Andjelkovic AV, 2005 Monocyte chemoattractant protein-1 regulation of blood-brain barrier permeability. J Cereb Blood Flow Metab 25, 593–606. [PubMed: 15689955]

Sulhan S, Lyon KA, Shapiro LA, Huang JH, 2020 Neuroinflammation and blood-brain barrier disruption following traumatic brain injury: Pathophysiology and potential therapeutic targets. J Neurosci Res 98, 19–28. [PubMed: 30259550]

Teler J, Tarnowski M, Safranow K, Maciejewska A, Sawczuk M, Dziedziejko V, Sluczanowska-Glabowska S, Pawlik A, 2017 CCL2, CCL5, IL4 and IL15 Gene Polymorphisms in Women with Gestational Diabetes Mellitus. Hormone and metabolic research = Hormon- und Stoffwechselforschung = Hormones et metabolisme 49, 10–15. [PubMed: 27472286]

Tolonen AM, Magga J, Szabo Z, Viitala P, Gao E, Moilanen AM, Ohukainen P, Vainio L, Koch WJ, Kerkela R, Ruskoaho H, Serpi R, 2014 Inhibition of Let-7 microRNA attenuates myocardial

Author Manuscript Author Manuscript Author Manuscript Author Manuscript

remodeling and improves cardiac function postinfarction in mice. Pharmacology research & perspectives 2, e00056. [PubMed: 25505600]

Uwamori H, Ono Y, Yamashita T, Arai K, Sudo R, 2019 Comparison of organ-specific endothelial cells in terms of microvascular formation and endothelial barrier functions. Microvasc Res 122, 60–70. [PubMed: 30472038]

Verma S, Nakaoke R, Dohgu S, Banks WA, 2006 Release of cytokines by brain endothelial cells: A polarized response to lipopolysaccharide. Brain Behav Immun 20, 449–455. [PubMed: 16309883]

Vlisides P, Mashour GA, 2016 Perioperative stroke. Canadian journal of anaesthesia = Journal canadien d'anesthesie 63, 193–204.

von Vietinghoff S, Ley K, 2009 IL-17A controls IL-17F production and maintains blood neutrophil counts in mice. J Immunol 183, 865–873. [PubMed: 19542376]

Wang X, Cao L, Wang Y, Wang X, Liu N, You Y, 2012 Regulation of let-7 and its target oncogenes (Review). Oncol Lett 3, 955–960. [PubMed: 22783372]

Wang Y, Bontempi B, Hong SM, Mehta K, Weinstein PR, Abrams GM, Liu J, 2008 A comprehensive analysis of gait impairment after experimental stroke and the therapeutic effect of environmental enrichment in rats. J Cereb Blood Flow Metab 28, 1936–1950. [PubMed: 18628778]

Winter B, Juckel G, Viktorov I, Katchanov J, Gietz A, Sohr R, Balkaya M, Hortnagl H, Endres M, 2005 Anxious and hyperactive phenotype following brief ischemic episodes in mice. Biol Psychiatry 57, 1166–1175. [PubMed: 15866557]

Xie L, Li W, Hersh J, Liu R, Yang SH, 2018 Experimental ischemic stroke induces long-term T cell activation in the brain. J Cereb Blood Flow Metab, 271678X18792372.

Yang Q, Tong X, Schieb L, Vaughan A, Gillespie C, Wiltz JL, King SC, Odom E, Merritt R, Hong Y, George MG, 2017a Vital Signs: Recent Trends in Stroke Death Rates - United States, 2000–2015. MMWR Morb Mortal Wkly Rep 66, 933–939. [PubMed: 28880858]

Yang S, Jin H, Zhu Y, Wan Y, Opoku EN, Zhu L, Hu B, 2017b Diverse Functions and Mechanisms of Pericytes in Ischemic Stroke. Curr Neuropharmacol 15, 892–905. [PubMed: 28088914]

Zhang C, 2008 The role of inflammatory cytokines in endothelial dysfunction. Basic Res Cardiol 103, 398–406. [PubMed: 18600364]

Zhang H, Xiong X, Gu L, Xie W, Zhao H, 2018 CD4 T cell deficiency attenuates ischemic stroke, inhibits oxidative stress, and enhances Akt/mTOR survival signaling pathways in mice. Chinese Neurosurgical Journal 4, 32.

Zhang L, Schallert T, Zhang ZG, Jiang Q, Arniego P, Li Q, Lu M, Chopp M, 2002 A test for detecting long-term sensorimotor dysfunction in the mouse after focal cerebral ischemia. J Neurosci Methods 117, 207–214. [PubMed: 12100987]

Zhang L, Yang J, Xue Q, Yang D, Lu Y, Guang X, Zhang W, Ba R, Zhu H, Ma X, 2016 An rs13293512 polymorphism in the promoter of let-7 is associated with a reduced risk of ischemic stroke. Journal of thrombosis and thrombolysis 42, 610–615. [PubMed: 27530126]

Zhang M, Martin BR, Adler MW, Razdan RK, Jallo JI, Tuma RF, 2007 Cannabinoid CB(2) receptor activation decreases cerebral infarction in a mouse focal ischemia/reperfusion model. J Cereb Blood Flow Metab 27, 1387–1396. [PubMed: 17245417]

Author Manuscript Author Manuscript Author Manuscript Author Manuscript

Highlights

- let-7g* preserves BBB integrity both *in vitro* and *in vivo*
- let-7g* attenuates neuroinflammation after stroke by reducing microglia activation
- brain neutrophil and T-cell infiltration are diminished in let-7-treated mice
- let-7g* decreases neuronal death after tMCAO
- increased locomotion and improved gait were found in mice treated with let-7g*

Author Manuscript Author Manuscript Author Manuscript Author Manuscript

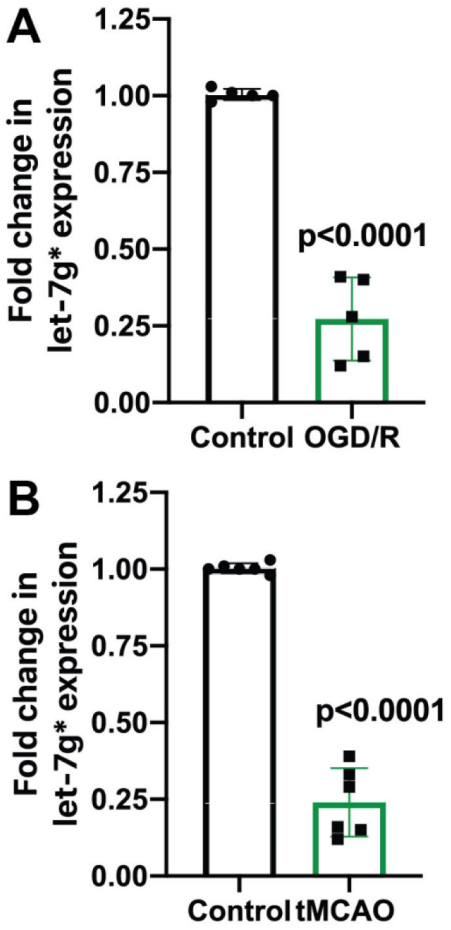

Figure 1. Ischemia/reperfusion conditions cause significant reduction in let-7g* miRNA expression.

qPCR analysis of let-7g* expression in BMVEC (A) and microvessels (B). BMVEC were subjected to 3 hr of OGD and 24 h reperfusion. Mice were subjected to 60 min ischemia and 24 h reperfusion performed as described in Materials and Methods. Microvessels from the ischemic part of the brain were isolated, miRNA extracted and analyzed in triplicate by qPCR. Results are presented as mean±SD from at least two independent experiments (n=4).

Author Manuscript Author Manuscript Author Manuscript Author Manuscript

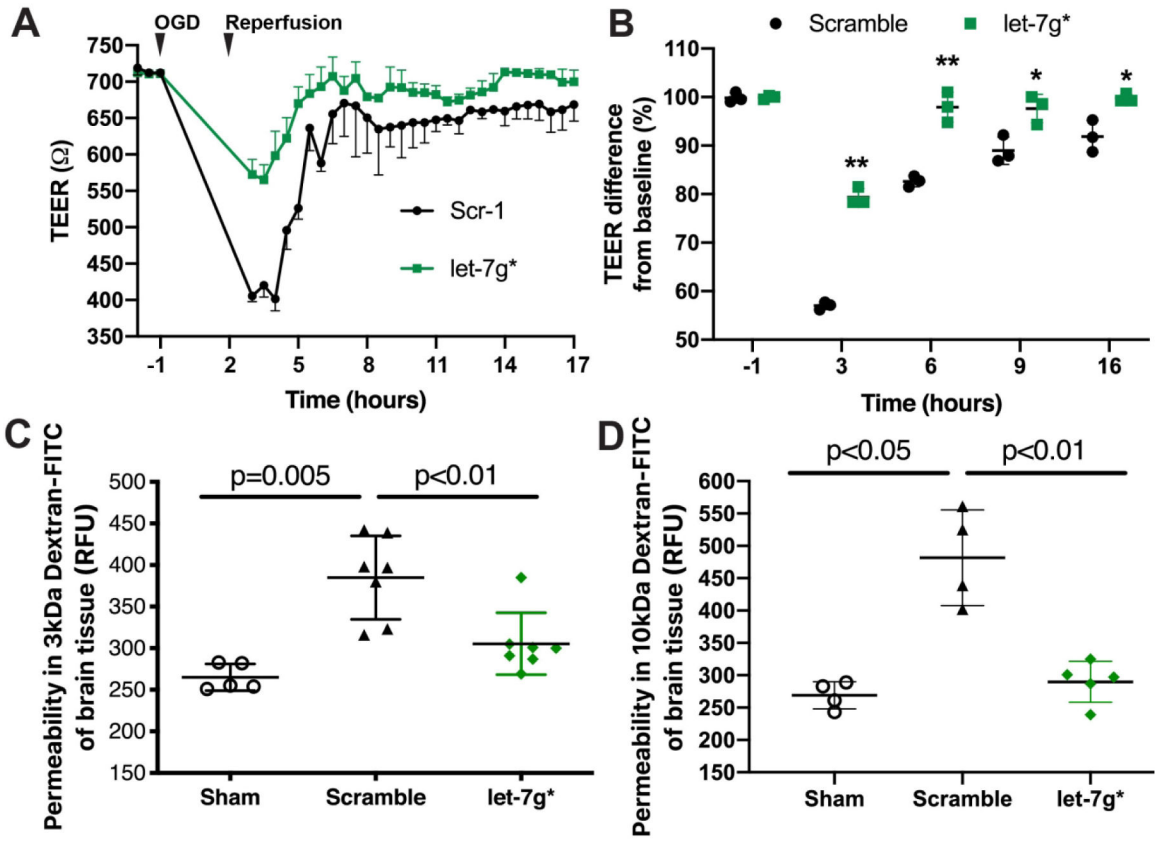

Figure 2. Overexpression of let-7g* attenuates BBB disruption.

Mimic oligos of let-7g* or non-coding (scramble) were transfected into endothelial cells. A. Absolute level of TEER (in ohms, Ω) after transfection of let-7g* or scramble miRNAs. B. Quantification of the difference in percent change in TEER at −1, 3, 6, 9, and 16 h of OGD/R. Results are presented as an average from at least two independent experiments (*p<0.05 or **p<0.01 *vs.* scramble control) consisting of at least 3 replicates. Mice were subjected to tMCAO and injected (i.v.) with liposome/exogenous miRNA complexes of mimic oligos of let-7g*, non-coding (NC=scramble), or vehicle only, with sham serving as the control. Quantification of FITC-labeled dextran 3kDA (C) or 10kDa (D) accumulation and representative images of each section of the brain are shown for each treatment group (sham control, scramble, let-7g*). Experiments were performed in triplicate with 4–7 mice in each group. Permeability is represented as mean fluorescence ± SD.

Author Manuscript Author Manuscript Author Manuscript Author Manuscript

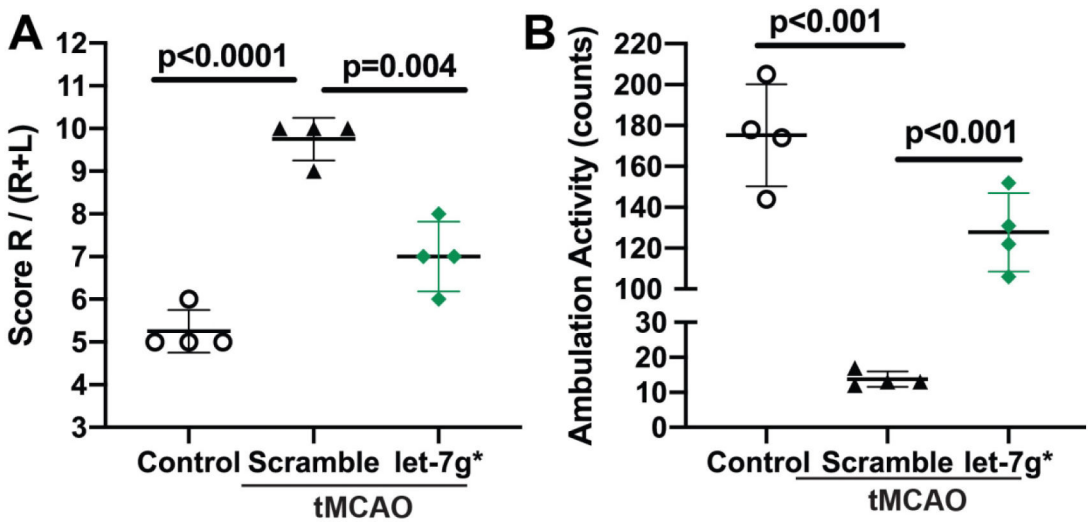

Figure 3. let-7g* expression improves neurological scores in tMCAO.

let-7g* was injected at specified times (2 and 24 h) following tMCAO as described (Bernstein et al., 2019). Sham vehicle only or scramble (NC) were injected as negative controls. Total ambulation activity test (A) and Corner test (B) were acquired prior to surgery and after reperfusion following ischemia. Results are presented as mean±SD from 4 mice per condition. #p<0.05 *vs.* non-specific miRNA control.

Author Manuscript Author Manuscript Author Manuscript Author Manuscript

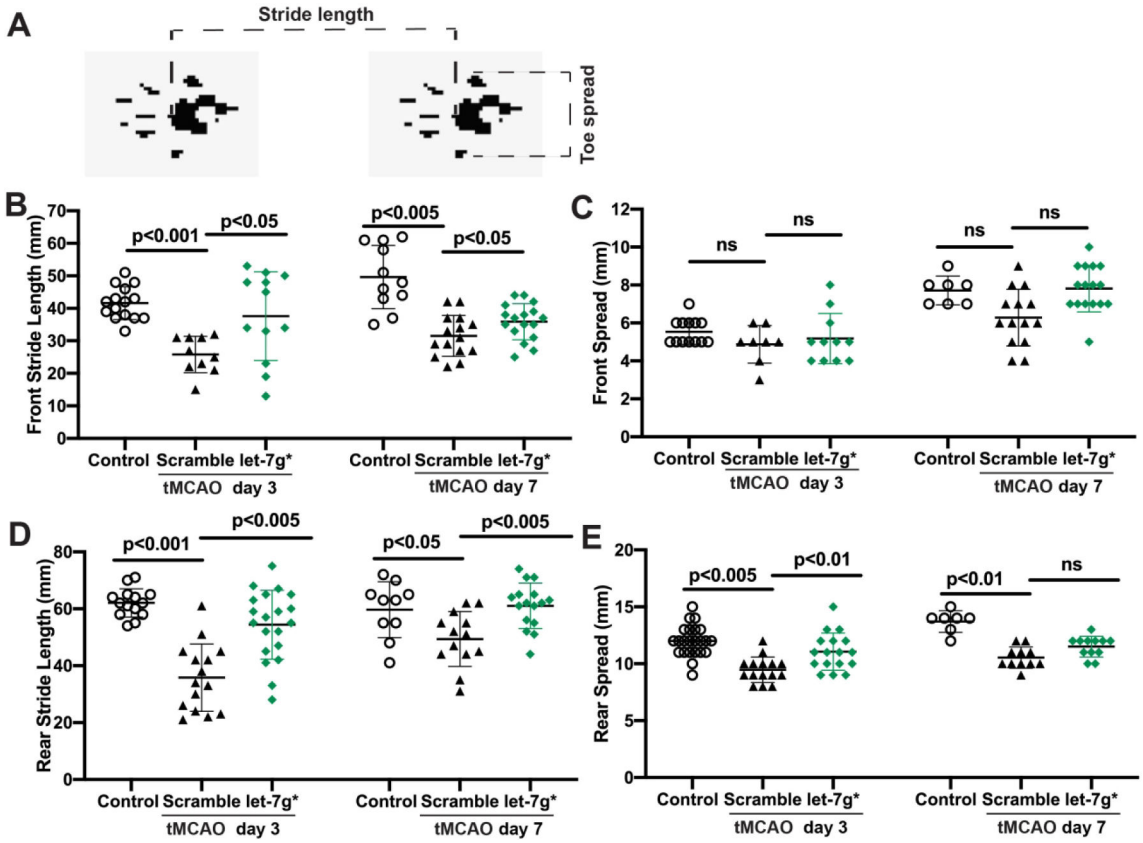

Figure 4. let-7g* expression recovers gait impairment after tMCAO.

Mice were subjected to tMCAO and injected with let-7g* or scramble (negative control oligo) or sham (vehicle only). Gait analysis was performed at 3- and 7-days post-stroke as described in Methods. A. Schematic of gait analysis by foot print. Quantification evaluation of front (B) and rear (D) foot stride, or front (C) and rear (E) foot spread was performed on mice, and presented as mean±SD from 7–14 mice per condition.

Author Manuscript
Author Manuscript
Author Manuscript
Author Manuscript

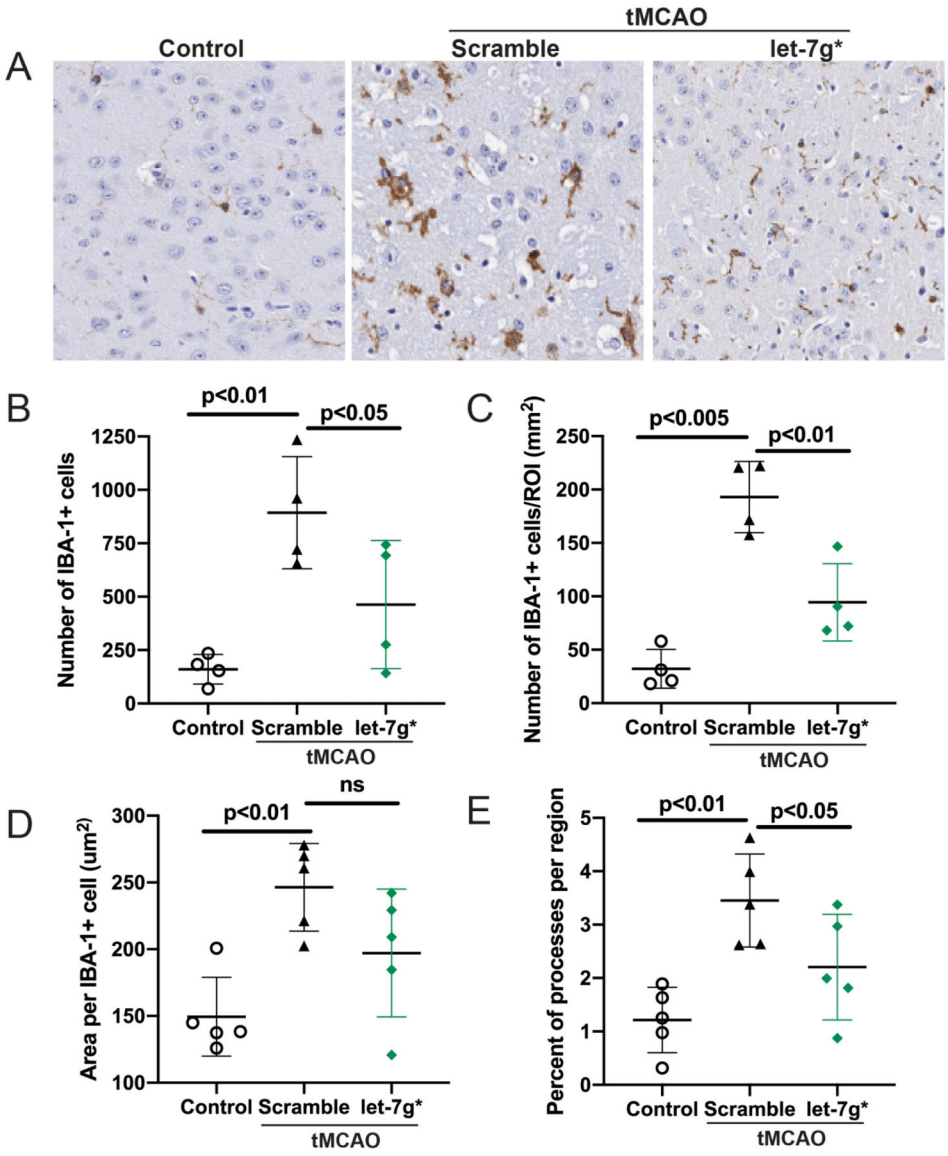

Figure 5. let-7g* overexpression lessens microglia activation after tMCAO.

Mice were subjected to tMCAO and treated with liposome/exogenous miRNA complexes of mimic oligos of let-7g*, non-coding (NC=scramble), or vehicle only. Microglial activation was measured by IBA staining by immunohistochemistry. A. Representative images of immunohistochemistry of IBA in brain sections, shown at 20X. Quantitative analysis of IBA-1 positive cells per field (B) or region of interest (ROI)(C), area per each IBA-1+ cell (D) and percent of processes per ROI (E) are presented. Data are shown as mean ±SD.

Author Manuscript Author Manuscript Author Manuscript Author Manuscript

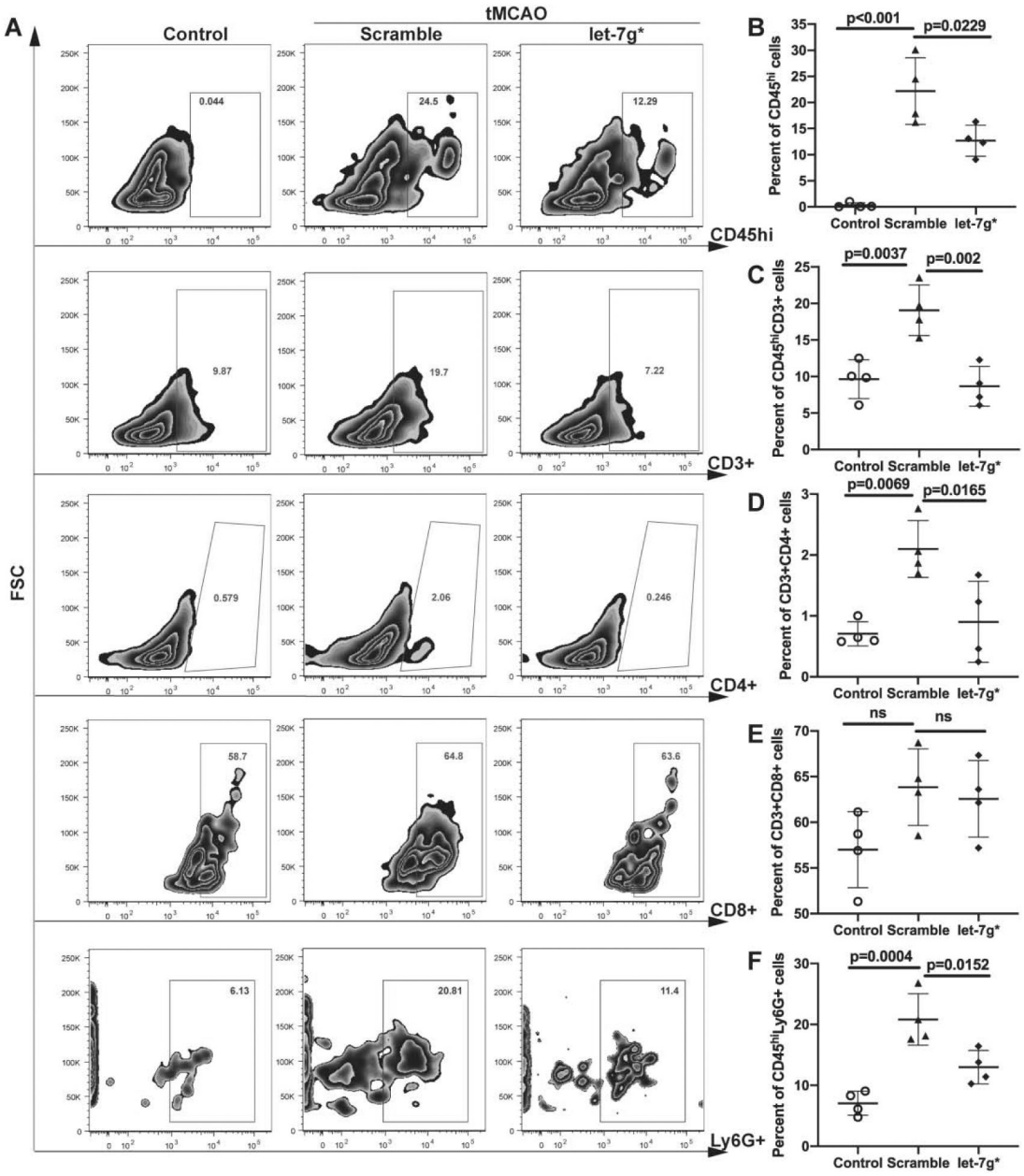

Figure 6. let-7g* expression reduces CNS infiltration of neutrophils and T cells after tMCAO.

Mice were subjected to tMCAO and treated with liposome/exogenous miRNA complexes of mimic oligos of let-7g*, non-coding (NC=scramble), or vehicle only. Flow cytometry analysis of BILs isolated from infarcted hemisphere (n=4). BILs were stained for CD45, CD3, CD4, CD8 and Ly6G markers. 10,000 events were recorded per tube. A. Representative FACS plots for above mentioned markers. Data are presented as mean ±SD for $CD45^{hi}$ cells (B), $CD45^{hi}CD3^{+}$ T cells (C), $CD45^{hi}CD3^{+}CD4^{+}$ (D) and $CD45^{hi}CD3^{+}CD8^{+}$ T cells (E), and $CD45^{hi}Ly6G^{+}$ neutrophils (F).

Author Manuscript Author Manuscript Author Manuscript Author Manuscript

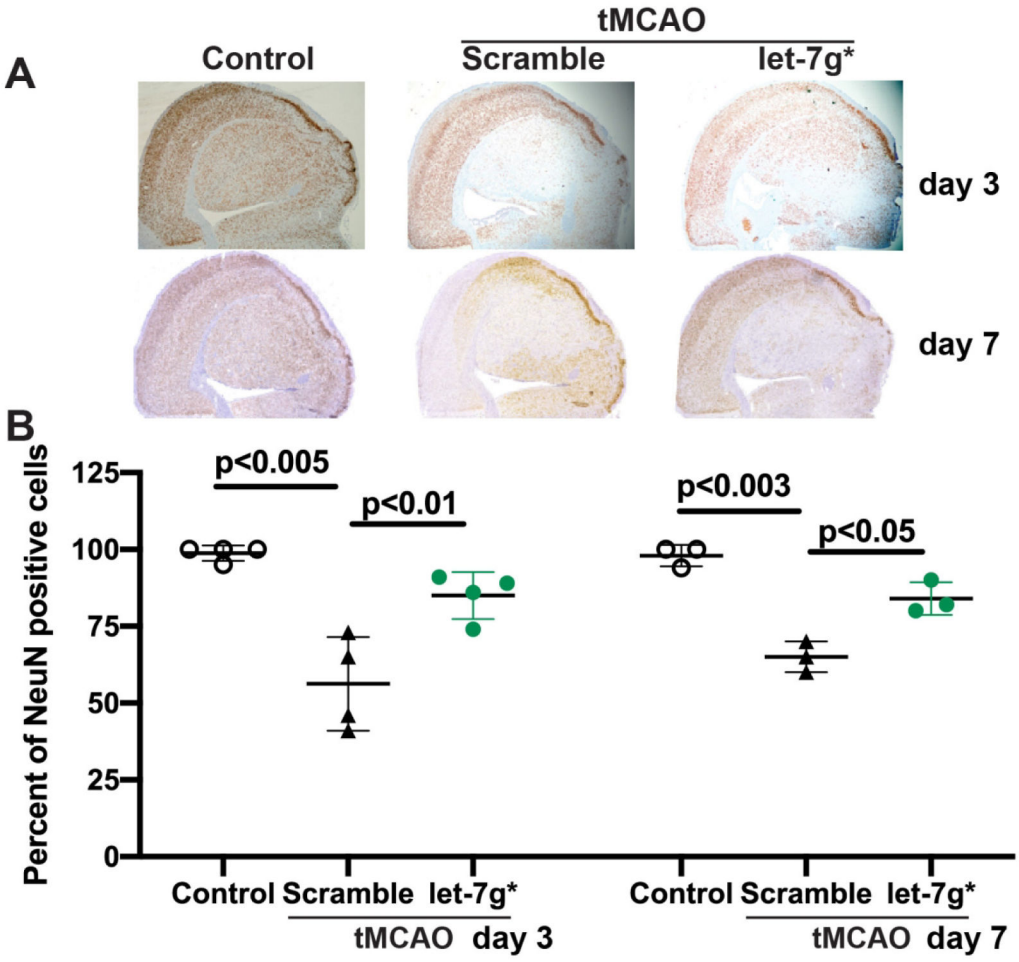

Figure 7. let-7g* overexpression prevents neuronal death after tMCAO.

Mice were subjected to tMCAO and treated with liposome/exogenous miRNA complexes of mimic oligos of let-7g*, non-coding (NC=scramble), or vehicle only. A. Representative images of immunohistochemistry of NeuN in brain sections, shown at 20X. B. Data are presented as mean ±SD.